

## **Experimental Section**

Solid-state synthesis of the precursor of Zn(OH)<sub>2</sub> nanostructures were as described in our previous report:[1] powders of Zn(NO<sub>3</sub>)<sub>2</sub>•6H<sub>2</sub>O and NaOH were placed in an agate mortar and ground at room temperature for 30 minutes. After adding 100 mL of distilled water, the products was centrifuged to remove Na<sup>+</sup> and excess alkali. Then the precipitation was dispersed into 50 mL deionized water by means of ultrasonic irradiation. The slurry has finally been achieved after repeating three times of the two steps. And then we used the doctor blade technique to uniformly spread a small amount of the slurry onto FTO conductive glass. By using the low-temperature plasma instrument (DT03S, Suzhou OPS Plasma Technology Co., Ltd) to treat the prepared anode in air after dried naturally for 12 h, the sample was then annealed at 200°C at a ramping rate of 1°C/min for 2 h and marked as ZnO-*x* which *x* replaces the treatment time. In this paper, a series of samples were prepared under the same conditions.

After annealing, the photoanode (5 mm × 5 mm) was subsequently sensitized with 0.5 mM Ruthenizer 535-bisTBA (N719) in absolute ethanol solution at 45 °C for 100 min to confirm that it was completely attached by dye molecules. Then the sample was carefully cleaned with wiping paper and washed with ethanol to remove unadsorbed dye before dried in a vacuum at room temperature. Platinized-sputtered FTO counter (PMC-5000 plasma multicoater) was used as the counter electrode. The redox electrolyte consisted of 0.06 M LiI, 0.6 M 1-butyl-3-methylimidazolium iodide, 0.03 M I<sub>2</sub>, 0.5 M 4-tert-butyl pyridine, and 0.1 M guanidinium thiocyanate. All chemicals were purchased from OPV Tech Co. Ltd.

The morphologies and structures of the samples were characterized by field-emission scanning electron microscopy (SEM; S-4800, Hitachi, Japan), N<sub>2</sub> adsorption-desorption isotherms (ASAP 2020 Analyzer, Micromeritics, USA). Phase identification was investigated by X-ray diffraction patterns (XRD; M18XCE, Bruker, Germany) using Cu K $\alpha$  radiation. Current–potential curves (J-V curves) were measured by linear sweep voltammetry using an electrochemical workstation(CHF-XM-500W, BeijingChangtuo Co., Ltd., Beijing, China) under the AM 1.5 standard (100mW cm<sup>-2</sup>) irradiation. The light intensity was calibrated with a standard Si photodiode detector(CEL-RCCN, Beijing Zhongjiaojinyuan Technology Co., Ltd., Beijing, China). Electrochemical impedance spectroscopy (EIS) analysis was performed with an electrochemical workstation (IM6, ZAHNER) in darkness with an AC signal of 20 mV in amplitude and the swept frequency range was from 100 mHz to 100kHz. Spectra analysis was performed using Zview modeling software.

## **Influence of power on the photoanodes**

We have tested the performances of the samples under different powers, J-V curves and the PCE were as shown in Figure S1 and Table S1.

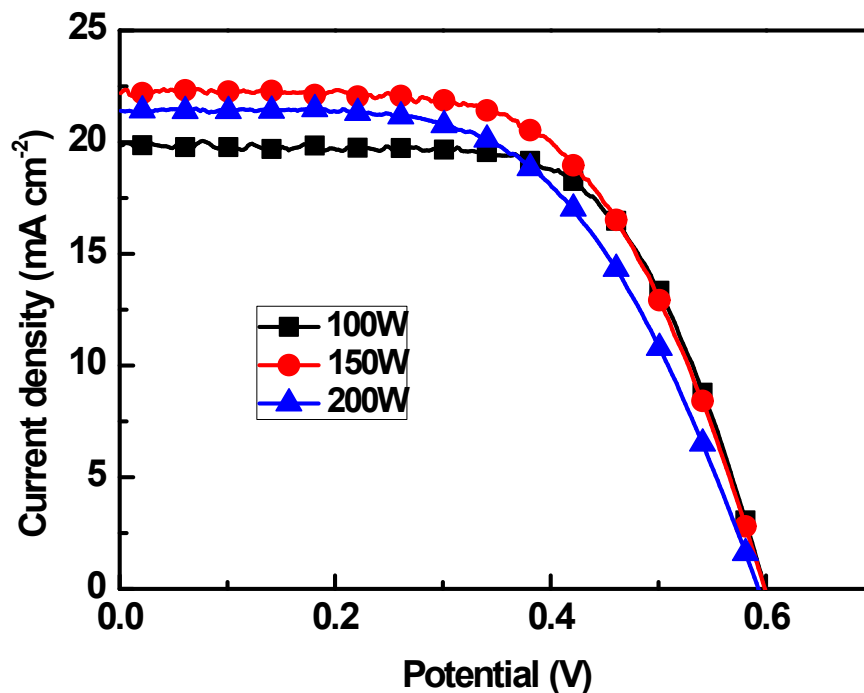


Figure S1. J-V curves of DSSCs based on different photoanodes, which were treated under different powers.

Table S1. PCE of DSSCs with photoanodes under different powers.

Power(watts)	200	150	100
PCE(%)	7.24	8.03	7.71

As shown in Figure S1, the photoelectric conversion efficiency reached the maximum value when under 150 watts. To more thoroughly study the influence of power, we carried out analysis on infrared spectrum. See Figure S2 below:

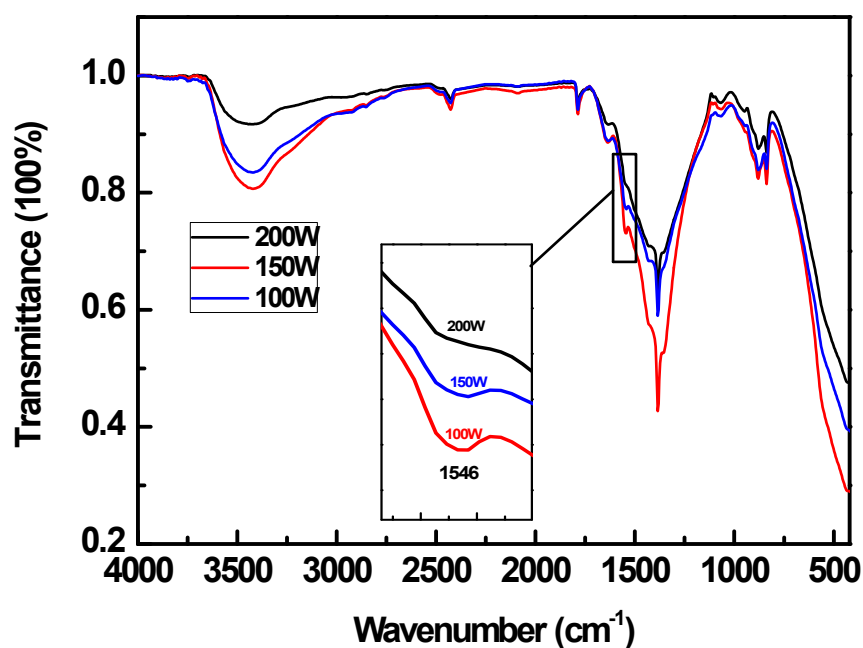


Figure S2. IR spectrum of ZnO film under different powers.

As clearly shown in Figure S2, the peak intensity of water molecules decreased with the increase of power, thus under lower power, water in the precursor could not be effectively removed, leading to more hydrogen defects in zinc oxide, which would hinder the improvement of PCE. Furthermore, it could be said that the power also had an influence on the crystallinity of the samples. Taking a close look at the X-ray diffraction (XRD) patterns in Figure S3 and the crystallinity in Table S2 by fitting from the results using analysis software Jade:

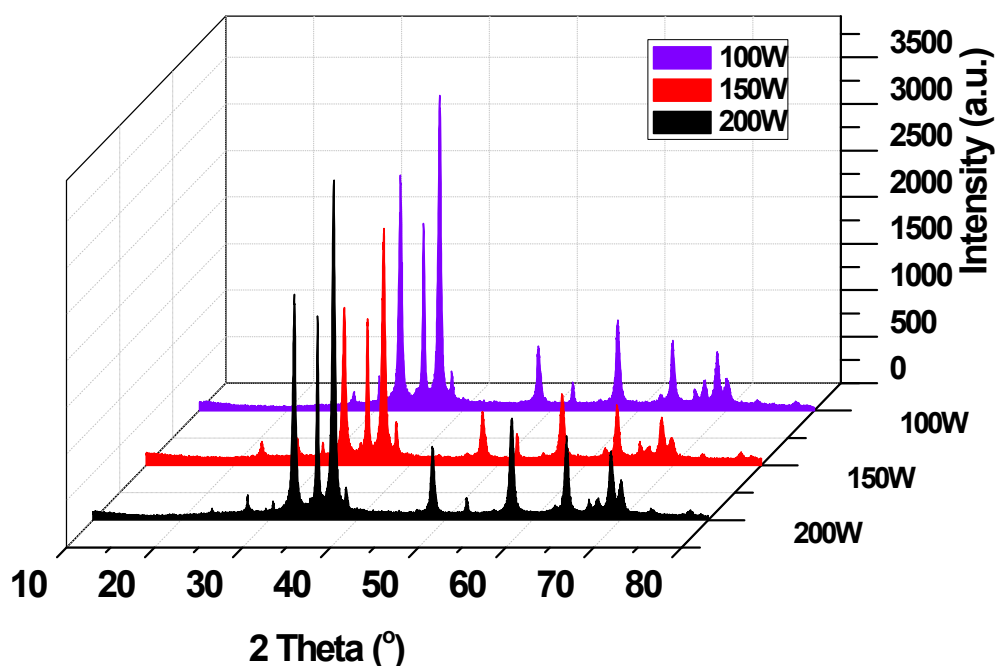


Figure S3. X-ray diffraction (XRD) patterns of ZnO film under different powers.

Table S2. Crystallinity of of ZnO film under different powers.

Power (watts)	200	150	100
Crystallinity from XRD (%)	9.05	13.85	14.19

It was clearly that the higher the power, the worse the degree of crystallinity. To ensure the results we had achieved, pictures of the electrode plate under different powers were taken and shown in Figure S4, the light from the corona charge on the electrode plate became stronger with the increase of power, which indicated that under high power, more high energy particles would be produced by the collision of air molecular. Therefore, combing with our precious study, it is believed that the sample should be treated under an appropriate power.

Figure S4. Electrode plate under different powers.

## EIS Fitting

According to the reference[2], The equivalent circuit is shown below:

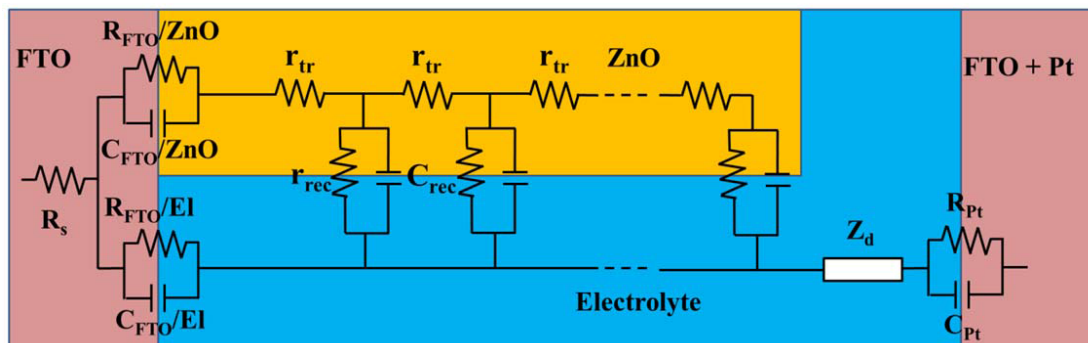
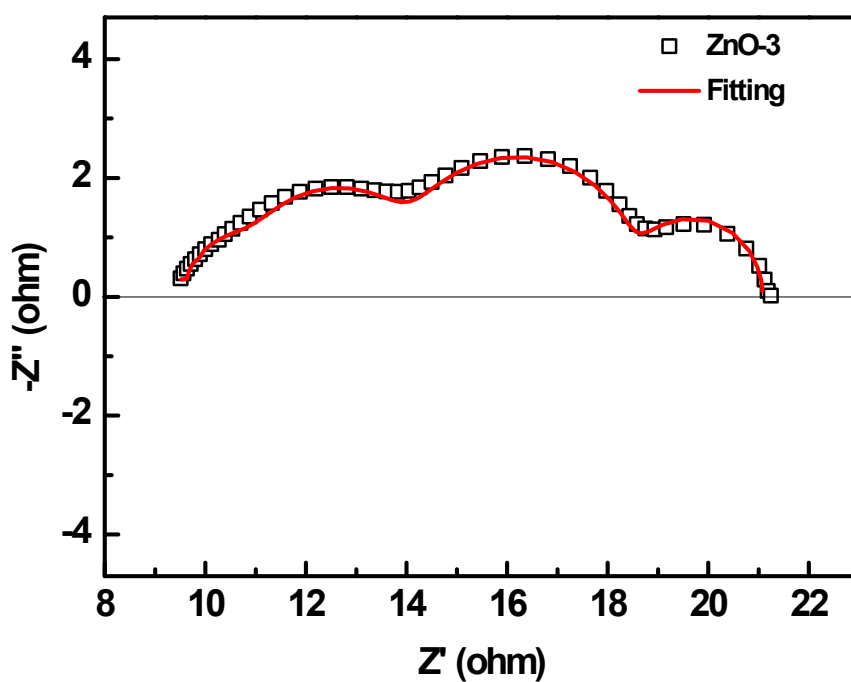


Figure S5. The equivalent circuit diagram of the dye sensitized solar cell (from Yantao Shi, et al., Adv. Mater., 2013, 25, 4413-4419).

In the picture,  $r_{tr}$  represents the electron transport resistance in ZnO film;  $R_s$  is the series resistance, including the contact resistance between the FTO glass and the zinc oxide film.

Take the sample ZnO-3 as example, the fitting line is almost overlapped with the original data, as shown below:



## Crystallinity from XRD

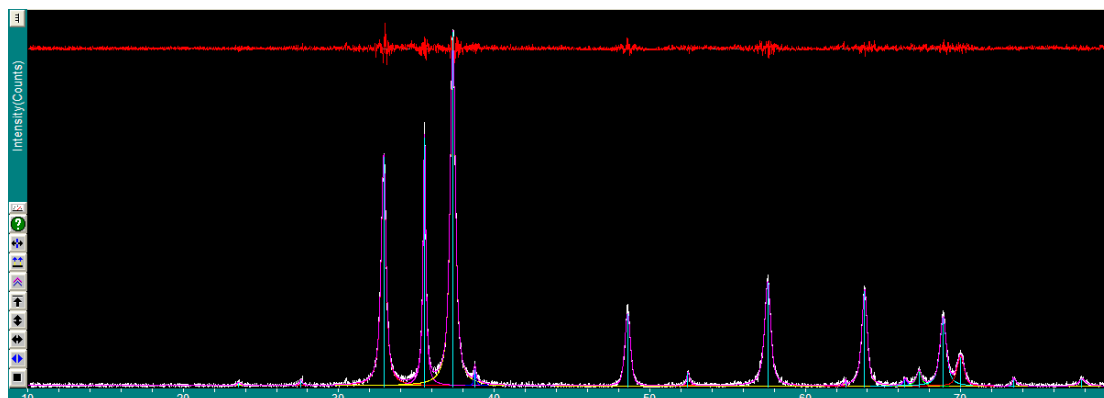


Figure S6. Fitting result of XRD pattern.

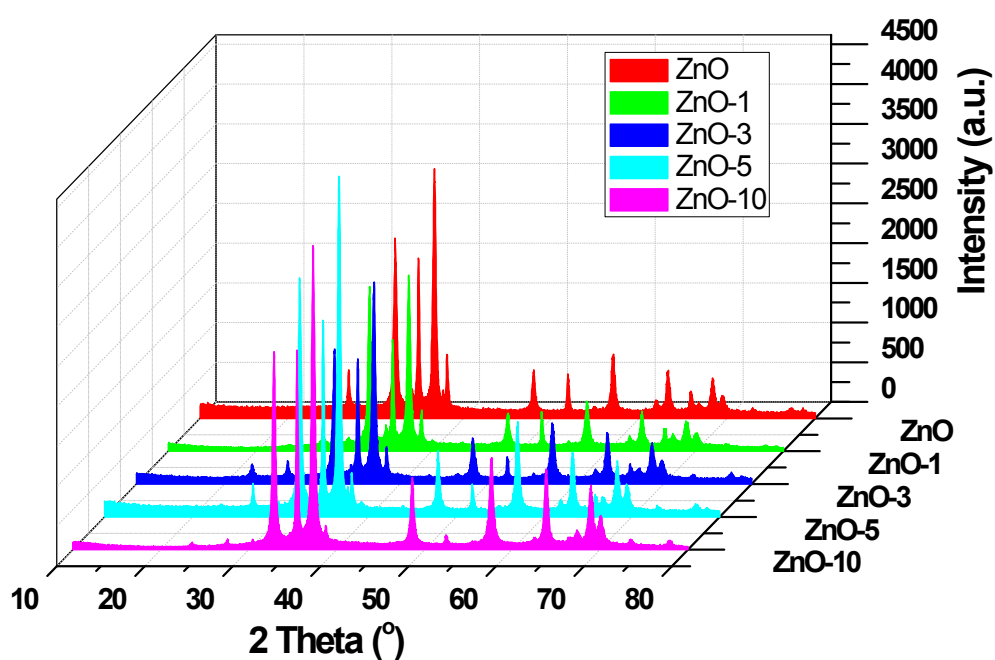


Figure S7. XRD spectrum of different samples.

## Analysis of specific surface

Seen from the table, after treated by air plasma, the specific surface area had a relatively small increase with time going by and reached the maximum value when treating 3 min. It was thought that during the process of treatment, the specific surface

area of the precursor has a very slight corrosion. The variation trend of the specific surface area was consistent with the variation trend of dye adsorption, moreover, though this change could increase the adsorption of dyes to a certain extent, it is not the main factor affecting the final efficiency.

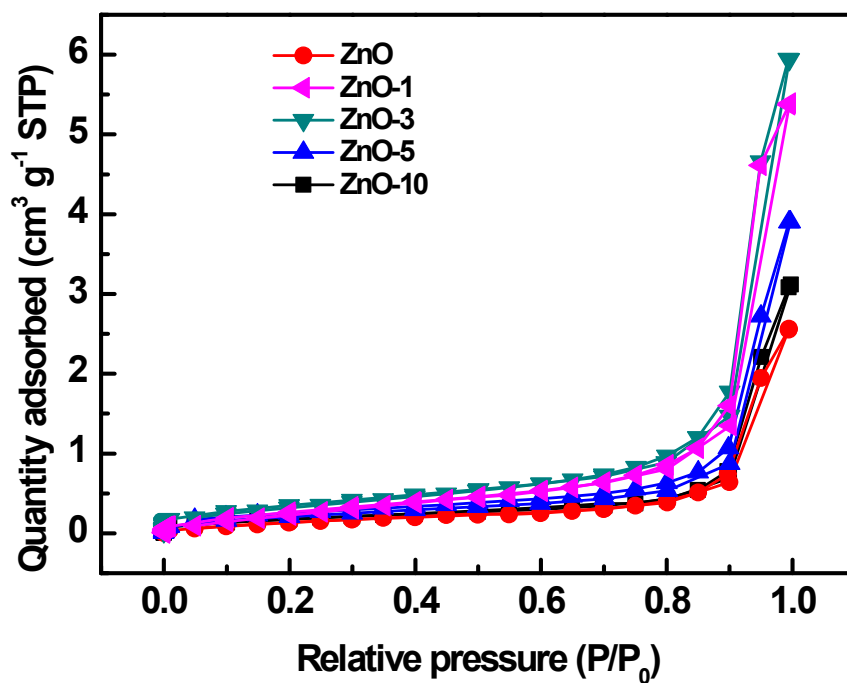


Figure S8. BET isotherm linear plots of the four samples.

Table S3. BET specific surface area and porosity of samples

Samples	$S_{\text{BET}}^{\text{a}}$ ( $\text{m}^2 \text{g}^{-1}$ )	$V_{\text{t}}^{\text{b}}$ ( $\text{cm}^3 \text{g}^{-1}$ )	$D_{\text{ap}}^{\text{c}}$ (nm)
ZnO	31.186	0.241	30.485
ZnO-1	37.783	0.250	30.362
ZnO-3	37.807	0.283	30.350
ZnO-5	34.215	0.231	30.471
ZnO-10	33.943	0.231	30.473

<sup>a</sup> BET specific surface area ( $S_{\text{BET}}$ ). <sup>b</sup> Total pore volume at  $P/P_0=0.99$  ( $V_{\text{t}}$ ). <sup>c</sup> Adsorption average pore width ( $D_{\text{ap}}=4V_{\text{t}}/S_{\text{BET}}$ ).

## References

- [1] J. Hu, Y. H. Xie, T. Bai, C. Y. Zhang, J. D. Wang, *J. Power Sources*, 2015, **286**, 175.
- [2] Y. T. Shi, K. Wang, Y. Du, H. Zhang, J. F. Gu, C. Zhu, L. Wang, W. Guo, A. Hagfeldt, N. Wang, T. L. Ma, *Adv. Mater.*, 2013, **25**, 4413.

